J Inorg Organomet Polym (2013) 23:1159–1171
DOI 10.1007/s10904-013-9908-8

Synthesis of Metal-Coordinated Poly(azomethine-urethane)s: Thermal Stability, Optical and Electrochemical Properties

Musa Kamacı · İsmet Kaya

Received: 24 January 2013 / Accepted: 5 July 2013 / Published online: 14 July 2013

Abstract In this study, the novel thermally stable metal-coordinated-poly(azomethine-urethane)s (PAMU-M)s were synthesized to investigate some physical properties such as thermal stability, optical and electrochemical properties. For this reason, we firstly synthesized the Schiff base via condensation reaction of *p*-phenylenediamine with 2,4-dihydroxy benzaldehyde. Secondly, metal-coordinated Schiff bases were synthesized by coordination reaction of the obtained Schiff base and different metal ions such as Cu(II), Ni(II), Pb(II) and Zn(II). Then, these metal-coordinated Schiff bases were converted to their PAMU derivatives by the step-polymerization reaction using 2,4-toluenediisocyanate. Also, thermal stability, electrochemical and optic properties of the obtained materials were investigated.

Keywords Thermal properties · Optical properties · Luminescence · Electrochemical properties · Polymers–metals

1 Introduction

Over the past years, metal-coordinated Schiff bases have become increasingly important owing to their unusual properties [1]. They are important class of ligands in coordination chemistry due to they readily form stable complexes with most of the transition metals [2]. Furthermore, the increasing interest in the coordination chemistry is focused on the potential applications such as antimicrobial properties [3], biological activity [4], non-linear optics [5], photo physical studies [6], catalysis [7], materials chemistry [8], absorption and transport of oxygen [9].

Polyurethanes are the most versatile family of polymeric materials and they have considerable potential to create new materials which are applicable in a wide range [10] such as coating [11], adhesives [12], sealants [13] and elastomer [14]. Also, poly(azomethine-urethane) derivatives of polyurethanes have been reported in the literature, and clarified their thermal stability [15], semicrystalline behavior [16], optical properties [17], and liquid crystalline properties [18]. Furthermore, their metal complexes have been also reported in the literature and clarified their biocidal activities [19], geometric structures [20], mechanical properties [21] and antimicrobial properties [22]. However, to the best our knowledge, there is no report on investigation of the optical, electrochemical and thermal properties of metal-coordinated poly(azomethine-urethane)s (PAMU-Ms).

In this paper, we synthesized the novel PAMU-Ms. The synthesis procedure contains three steps: The first step consists of condensation reaction of 2,4-dihydroxy benzaldehyde (2,4-DHB) with *p*-phenylenediamine (PDA) to form Schiff base. The second step consists of coordination reaction of the obtained Schiff base with different metal ions such as Cu(II), Ni(II), Pb(II) or Zn(II) to form metal-coordinated materials. The last step consists of PAMU forming which is a simple the step-polymerization reaction occurs between 2,4-toluenediisocyanate (TDI) with preformed metal-coordinated Schiff bases to obtain PAMU-M kinds. We characterized the obtained materials using FT-IR, ^{1}H NMR, ^{13}C NMR, SEC, TG–DTA and DSC techniques. We also

M. Kamacı
Department of Chemistry, Kamil Özdağ Science Faculty, Karamanoğlu Mehmetbey University, 70100 Karaman, Turkey

M. Kamacı · İ. Kaya (✉)
Polymer Synthesis and Analysis Laboratory, Department of Chemistry, Faculty of Sciences and Arts, Çanakkale Onsekiz Mart University, 17020 Çanakkale, Turkey
e-mail: kayaismet@hotmail.com

determined optical and electrochemical properties of the obtained materials using UV–Vis, CV and photo luminescence (PL) techniques.

2 Experimental

2.1 Materials

2,4-Dihydroxy benzaldehyde, *p*-phenylenediamine (PDA), $Cu(Ac)_2{\cdot}H_2O$, $Ni(Ac)_2{\cdot}4H_2O$, $Pb(Ac)_2{\cdot}3H_2O$, $Zn(Ac)_2{\cdot}2H_2O$, 2,4-toluenediisocyanate (TDI), dimethylformamide (DMF), dimethylsulfoxide (DMSO), tetrahydrofurane (THF), methanol (MeOH), ethanol (EtOH), acetone, acetonitrile, toluene, ethyl acetate, $CHCl_3$, CCl_4 and *n*-hexane were supplied from Merck Chemical Co. (Germany).

2.2 Synthesis of the Schiff Bases

Schiff base abbreviated as 2,4-DHB–PDA was synthesized by the condensation reactions of 2,4-dihydroxy benzaldehyde (2,4-DHB) with *p*-phylenediamine (PDA). Synthesis procedure of 2,4-DHB–PDA is as follows: 2,4-DHB (1.105 g, 8.00×10^{-3} mol) was dissolved in 50 mL methanol and added into a 250 mL three-necked round-bottom flask which was fitted with condenser, thermometer and magnetic stirrer. Reaction mixture was heated up to 50 °C and then PDA (0.433 g, 4.00×10^{-3} mol) in 20 mL methanol was added into the flask. Reaction was maintained for 3 h under reflux, and cooled at the room temperature. The obtained Schiff base was washed acetonitrile (2×50 mL) and water (2×100 mL) to remove the unreacted components [23]. The product was dried in a vacuum oven at 75 °C (yield 94 %).

2.3 Synthesis of the Metal-Coordinated Schiff Bases (2,4-DHB–PDA-Ms)

Metal-coordinated Schiff bases (2,4-DHB–PDA-Ms) abbreviated as 2,4-DHB–PDA–Cu, 2,4-DHB–PDA–Ni, 2,4-DHB–PDA–Pb and 2,4-DHB–PDA–Zn were synthesized by the coordination. Reactions were made as follow: 2,4-DHB–PDA (0.307 g, 8.81×10^{-4}) was placed into a 250 mL three-necked round-bottom flask which was fitted with condenser, thermometer and magnetic stirrer. 60 mL DMF/MeOH (1/3) mixture was added into the flask and reaction mixture was heated at 60 °C. A solution of $Cu(Ac)_2{\cdot}H_2O$ (0.175 g, 8.81×10^{-4} mol), $Ni(Ac)_2$ $4H_2O$ (0.219 g, 8.81×10^{-4} mol), $Pb(Ac)_2{\cdot}3H_2O$ (0.334 g, 8.81×10^{-4} mol) or $Zn(Ac)_2{\cdot}2H_2O$ (0.193 g, 8.81×10^{-4} mol) in 30 mL methanol were added into the flask and reaction mixtures were maintained for 3 h under reflux. The obtained materials were washed with toluene (2×100 mL) and water (2×100 mL), respectively, and dried in vacuum oven for 24 h [1]. The yields of 2,4-DHB–PDA–Cu, 2,4-DHB–PDA–Ni, 2,4-DHB–PDA–Pb and 2,4-DHB–PDA–Zn were found as 86, 84, 89 and 81 %, respectively.

2.4 Synthesis of the Metal-Coordinated Poly(azomethine-urethane)s (PAMU-Ms)

Preformed metal-coordinated Schiff bases were used in synthesis of the PAMU-Ms abbreviated as PU-2,4-DHB–PDA–Cu, PU-2,4-DHB–PDA–Ni, PU-2,4-DHB–PDA–Pb and PU-2,4-DHB–PDA–Zn. Synthesis procedure of PAMU-Ms are as follows: 2,4-DHB–PDA–Cu (0.512 g, 1.25×10^{-3} mol), 2,4-DHB–PDA–Ni (0.506 g, 1.25×10^{-3} mol), 2,4-DHB–PDA–Pb (0.692 g, 1.25×10^{-3} mol) or 2,4-DHB–PDA–Zn (0.515 g, 1.25×10^{-3} mol) were dissolved in 60 mL DMF/THF (1/3) mixture and added into a 250 mL three-necked round-bottom flask which was fitted with condenser, magnetic stirrer, and inert gas supplier. Reaction mixtures were heated up to 60 °C, TDI (0.436 g, 2.50×10^{-3} mol) was dissolved in 50 mL THF and added into the flask. Reactions were maintained for 6 h under Argon atmosphere, cooled at the room temperature and kept for 24 h. The obtained PAMU-Ms were washed by methanol (2×50 mL), acetonitrile (2×50 mL) and distilled water (2×100 mL) to remove the unreacted components. The products were dried in a vacuum oven at 75 °C for 24 h [24]. The yields of PU-2,4-DHB–PDA–Cu, PU-2,4-DHB–PDA–Ni, PU-2,4-DHB–PDA–Pb and PU-2,4-DHB–PDA–Zn were found as 90, 85, 80 and 83 %, respectively. All the synthesis procedures were summarized in Scheme 1.

2.5 Characterization Techniques

The solubility tests were carried out in different solvents by using 1 mg sample and 1 mL solvent at 25 °C. The infrared spectra were measured by Perkin Elmer FT-IR Spectrum one. The FT-IR spectra were recorded using universal ATR sampling accessory (4,000–550 cm^{-1}). ^1H and ^{13}C-NMR spectra (Bruker AC FT-NMR spectrometer operating at 400 and 100.6 MHz, respectively) were also recorded by using deuterated DMSO-d_6 as a solvent at 25 °C. Tetramethylsilane was used as internal standard. Thermal data were obtained by using Perkin Elmer Diamond Thermal Analysis. The TG–DTA measurements were made between 20 and 1,000 °C (in N_2, 10 °C/min). DSC analyses were carried out between 25 and 420 °C (in N_2, 20 °C/min) using Perkin Elmer Pyris Sapphire DSC. The number-average molecular weight (M_n), weight-average molecular weight (M_w) and polydispersity index (PDI) were determined by size exclusion chromatography (SEC) techniques of Shimadzu Co. For SEC investigations, an SGX (100 Å and 7 nm diameter loading material) 3.3 mm i.d. × 300 mm columns was used; eluent: DMF (0.4 mL/min), polystyrene standards

Scheme 1 Syntheses of 2,4-DHB–PDA, 2,4-DHB–PDA-Ms and PAMU-Ms

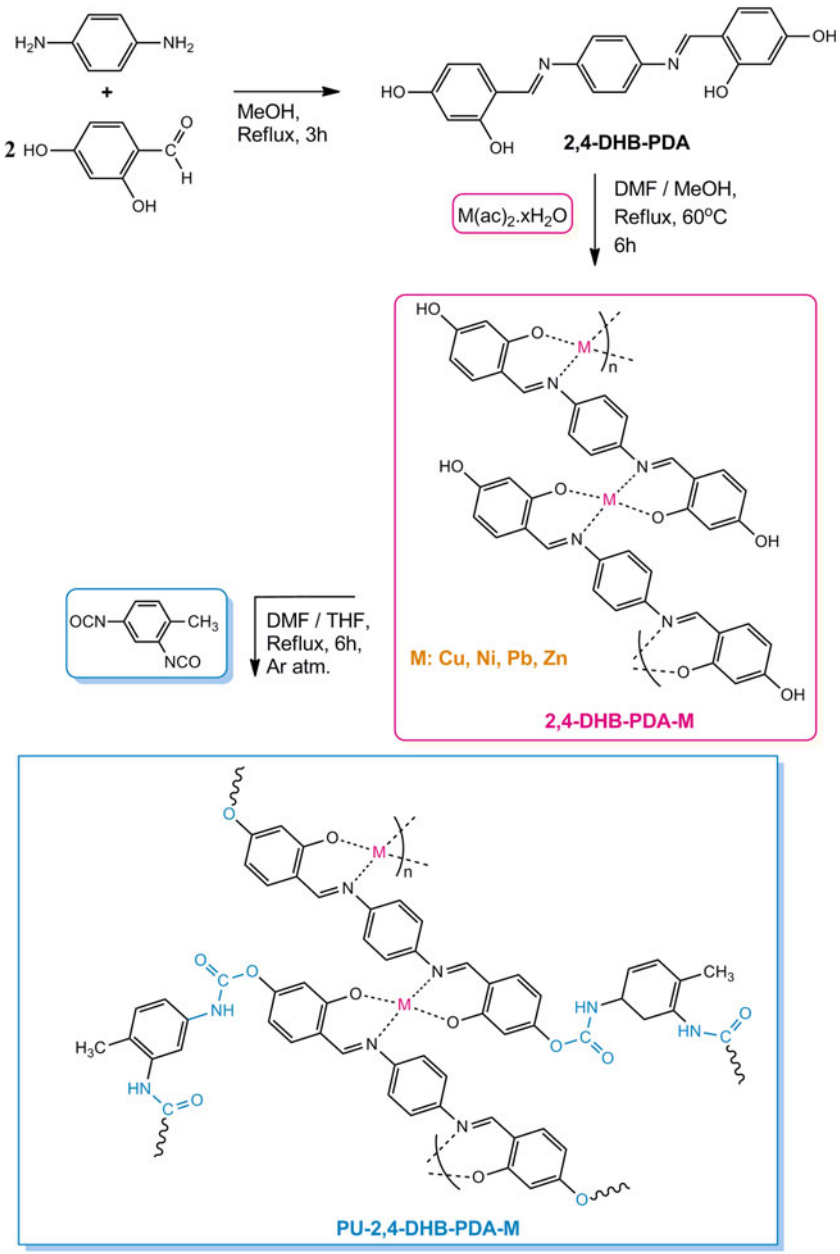

Table 1 Solubility test results of the synthesized materials

Compounds	MeOH	Acetone	Acetonitrile	$CHCl_3$	Toluene	Hexane	THF	DMF	DMSO
2,4-DHB–PDA	+	+	+	⊥	–	–	+	+	+
2,4-DHB–PDA–Cu	⊥	–	–	–	–	–	⊥	+	+
2,4-DHB–PDA–Ni	⊥	–	–	–	–	–	⊥	+	+
2,4-DHB–PDA–Pb	⊥	⊥	⊥	–	–	–	⊥	+	+
2,4-DHB–PDA–Zn	⊥	–	⊥	–	–	–	⊥	+	+
PU-2,4-DHB–PDA–Cu	⊥	–	–	–	–	–	⊥	+	+
PU-2,4-DHB–PDA–Ni	⊥	–	–	–	–	–	⊥	+	+
PU-2,4-DHB–PDA–Pb	⊥	–	–	–	–	–	⊥	+	+
PU-2,4-DHB–PDA–Zn	⊥	–	⊥	–	–	–	⊥	+	+

+ Soluble, – insoluble, ⊥ partly soluble

were used. Moreover, refractive index detector (RID) was used to analyze the products at 25 °C.

2.6 Optical and Electrochemical Properties

The optical band gaps (E_g) of the synthesized compounds were calculated from their absorption edges. Ultraviolet–visible (UV–Vis) spectra were measured by Perkin Elmer Lambda 25. The absorption spectra were recorded by using DMSO at 25 °C.

Cyclic voltammetry (CV) measurements were carried out with a CHI 660C Electrochemical Analyzer (CH Instruments, Texas, USA) at a potential scan rate of 20 mV/s. All the experiments were performed in a dry box filled with argon at room temperature. The electrochemical potential of Ag was calibrated with respect to the ferrocene/ferrocenium (Fc/Fc^+) couple. The half-wave potential ($E^{1/2}$) of (Fc/Fc^+) measured in 0.1 M tetrabutylammonium hexafluorophosphate ($TBAPF_6$) acetonitrile solution is 0.39 V with respect to Ag wire. The voltammetric measurements were carried out in acetonitrile, and DMSO [25]. An ultrasonic bath was used to solve the samples. The HOMO–LUMO energy levels and electrochemical band gaps (E'_g) were calculated from the oxidation and reduction onset values.

2.7 Fluorescence Measurements

A Shimadzu RF-5301PC spectrofluorophotometer was used in fluorescence measurements. Emission and excitation spectra of the synthesized compounds were obtained in solution forms in DMF. Measurements were made in a wide concentration range between 2.81×10^{-3} and 7.00×10^{-4} mg/L to determine the optimal fluorescence concentrations. Slit width in all measurements was 3 nm.

3 Results and Discussion

3.1 Solubilities and Structures of the Obtained Materials

The solubility test results are shown in Table 1. According to Table 1, the synthesized metal-coordinated Schiff bases and their poly(azomethine-urethane) derivatives are completely soluble only in strongly polar solvents like DMSO and DMF, partly soluble in methanol and THF while they are insoluble in $CHCl_3$, toluene and hexane. According to the Table 1, the synthesized Schiff base-metal complexes have higher solubilities compared to PAMU-Ms because of PAMU-Ms have higher molecular weights than the synthesized monomers.

Table 2 FT-IR spectrum data of synthesized compounds and starting materials

Compounds	Urethane –NH	Urethane –C=O	Imine –N=CH	Isocyanate –C=O	Isocyanate –C=N	–OH	$-NH_2$	M–O	Aldehyde –CHO	Aromatic –CH	Aliphatic –CH	Aromatic –C=C
2,4-DHB	–	–	–	–	–	3,098	–	–	1,708	3,040	–	1627, 1614, 1598
PDA	–	–	–	–	–	–	3,373	–	–	3,008	–	1580, 1548
TDI	–	–	–	2,234	1,615	–	–	–	–	3,041	2,924	1573, 1522
2,4-DHB–PDA	–	–	1,608	–	–	3,312	–	–	–	3,014	–	1547, 1503
2,4-DHB–PDA–Cu	–	–	1,603	–	–	3,292	–	660	–	3,011	–	1583, 1534
2,4-DHB–PDA–Ni	–	–	1,601	–	–	3,346	–	664	–	3,056	–	1601, 1543, 1503
2,4-DHB–PDA–Pb	–	–	1,599	–	–	3,334	–	656	–	3,048	–	1543, 1501
2,4-DHB–PDA–Zn	–	–	1,597	–	–	3,272	–	662	–	3,047	–	1539, 1510
PU-2,4-DHB–PDA–Cu	3,254	1,706	1,655	–	–	–	–	662	–	3,035	2,952	1585, 1531
PU-2,4-DHB–PDA–Ni	3,258	1,708	1,653	–	–	–	–	664	–	3,072	2,948	1596, 1530, 1500
PU-2,4-DHB–PDA–Pb	3,289	1,710	1,612	–	–	–	–	661	–	3,047	2,919	1598, 1506
PU-2,4-DHB–PDA–Zn	3,350	1,688	1,611	–	–	–	–	664	–	3,052	2,982	1547, 1507

FT-IR spectral data of the starting materials and the synthesized materials are summarized in Table 2. According to Table 2, characteristic aldehyde and hydroxyl (–OH) peaks of 2,4-dihydroxy benzaldehyde (2,4-DHB) are observed at 1,708 and 3,098 cm^{-1}, respectively. In the FT-IR spectral data of *p*-PDA $–NH_2$ peak is observed at 3,373 cm^{-1}. The structures of the synthesized Schiff base is confirmed by growing imine (–CH=N) peak with disappearing of the $–NH_2$ peak at PDA and the carbonyl (–C=O) peak of 2,4-DHB used in the condensation reactions. In the FT-IR spectral data of 2,4-DHB–PDA imine (–N=CH) and hydroxyl (–OH) peaks are observed at 1,608 and 3,312 cm^{-1}, respectively. As seen in Table 2, the structures of the metal-containing Schiff bases are confirmed by growing new peak between 656 and 664 cm^{-1} indicating metal–O (Cu–O, Ni–O, Pb–O and Zn–O) coordination bond and M-H_2O stretching vibrations between 977–990 (rocking) and 739–754 cm^{-1} (wagging) for coordinated water [26]. Imine (–N=CH) and hydroxyl (–OH) peaks of metal-coordinated Schiff bases are observed between 1,597–1,603 and 3,292–3,346 cm^{-1}, respectively. Also, azomethine stretching in the complexes is shifted towards the lower frequencies (5–9 cm^{-1}) as a result of coordination of the azomethine nitrogen atom to the metal ion [27]. According to FT-IR spectral data of TDI characteristic isocyanate –C=O and –C=N peaks are observed at 2,234 and 1,615 cm^{-1}, respectively, which agrees with the literature values [28]. According to Table 2, hydroxyl (–OH) group of Schiff base, –C=O and –C=N stretch vibrations of TDI disappear due to urethane formation. Moreover, in the FT-IR spectral data of PAMU-Ms the new peaks appear between 3,254–3,350 and 1,688–1,710 cm^{-1}, respectively, which could be attributed to urethane –NH and carbonyl (–C=O) stretch vibrations, respectively. Azomethine bonds (–N=CH) in the structures of PAMU-Ms are observed between 1,611 and 1,655 cm^{-1}, which are a bit lower than those of their metal-coordinated Schiff base due to the electron withdrawing effect of the urethane group in the polymer structures which decreases the electron density of imine carbon and consequently imine vibration [29]. Some additional peaks including aliphatic C–H (2,919–2,982 cm^{-1}) vibration and aromatic C–H (3,008–3,072 cm^{-1}) stretch, aromatic –C=C stretch (1,627–1,501 cm^{-1}) are also shown in Table 2. The

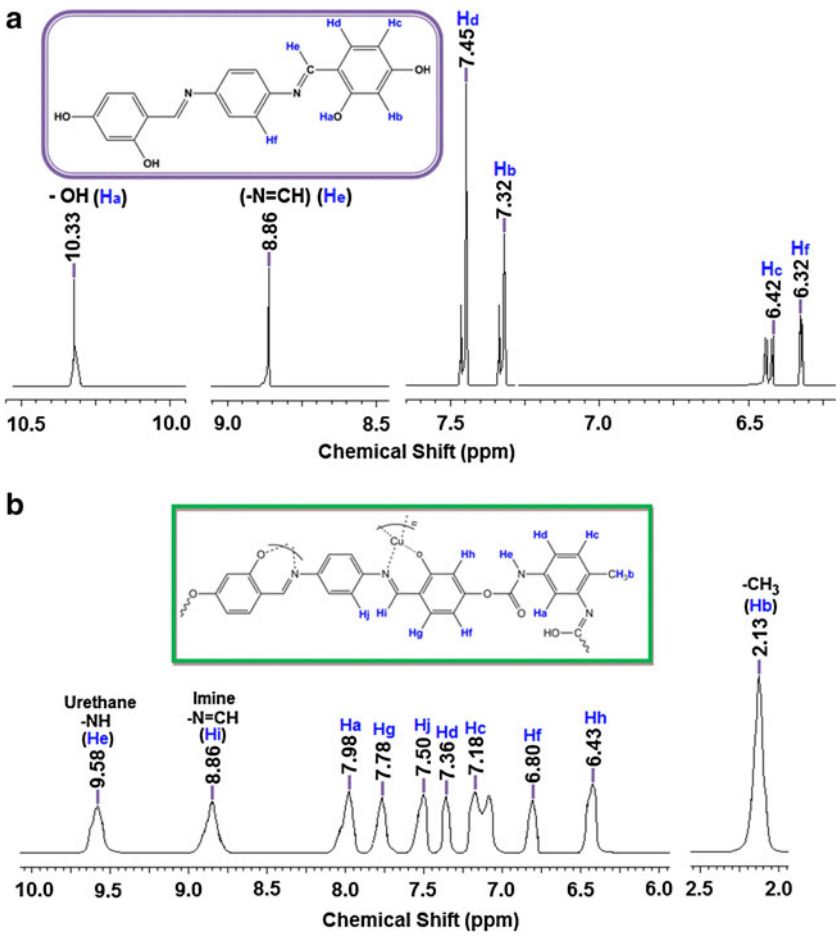

Fig. 1 ^{1}H-NMR spectra of 2,4-DHB–PDA (**a**) and PU-2,4-DHB–PDA–Cu (**b**)

Table 3 NMR spectra data of the obtained materials

Compounds	Spectral data (δ_{ppm})
2,4-DHB–PDA	*^{1}H-NMR (DMSO-d6)* 10.03 (–OH, H_a, s), 8.86 (–N=CH), H_e, s), 7.45 (Ar–H_d, d), 7.32 (Ar–H_b, d), 6.42 (Ar–H_c, d) and 6.32 (Ar–H_f, s)
	^{13}C-NMR (DMSO-d6) 163.04 (–OH, C_1-ipso), 162.02 (–OH, C_3-ipso), 157.17 (–HC=N, C_7-ipso), 146.10 (C_8), 134.43 (C_5–H), 122.11 (C_9–H), 112.13 (C_6), 107.93 (C_4–H) and 102.39 (C_2–H)
	^{1}H-NMR (DMSO-d6) 9.96 (–OH, H_b, s), 8.42 (–N=CH), H_e, s), 7.67 (Ar–H_d, d), 7.31 (Ar–H_f, m), 7.63 (Ar–H_b, s), 6.45 (Ar–H_a, s) and 6.39 (Ar–H_c, d)
2,4-DHB–PDA–Cu	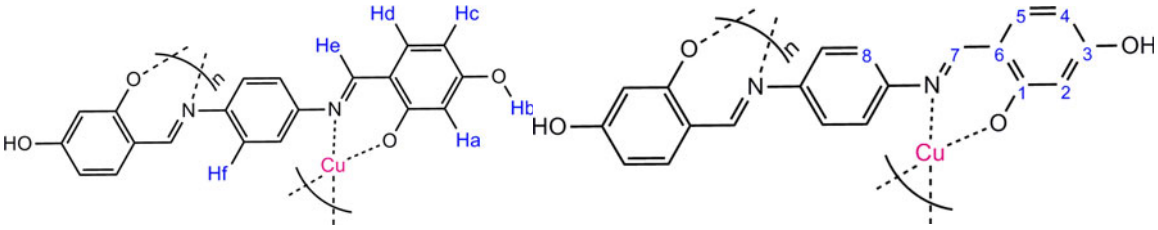
	^{13}C-NMR (DMSO-d6) 163.70 (–OH, C_3-ipso), 160.26 (–HC=N, C_7-ipso), 157.82 (C_1), 133.45 (C_5–H), 124.63 (C_8–H), 112.60 (C_6), 108.34 (C_4–H) and 102.93 (C_2–H)
	^{1}H-NMR (DMSO-d6) 9.58 (Urethane (–NH), H_e, s), 8.86 (–N=CH, H_i, s), 7.98 (Ar–H_a, s), 7.78 (Ar–H_g, s), 7.50 (Ar–H_j, s), 7.36 (Ar–H_d, s), 7.18 (Ar–H_c, d), 6.80 (Ar-H_f, s), 6.43 (Ar–H_h, s) and 2.13 (–CH_3, H_b, s)
PU-2,4-DHB–PDA–Cu	*^{13}C-NMR (DMSO-d6)* 162.39 (–N=CH, C_{15}-ipso), 154.72 (Urethane, (–C=O), C_8-ipso), 153.95 (C_{13}), 148.70 (C_9), 144.62 (C_{16}), 137.10 (C_2), 136.40 (C_7), 133.49 (C_{11}–H), 130.21 (C_3), 125.51 (C_5–H), 121.36 (C_{17}–H), 117.78 (C_6–H), 115.41 (C_{12}), 113.61 (C_{10}–H), 110.36 (C_1–H), 105.25 (C_{14}–H) and 17.14 (–CH_3, C_4)

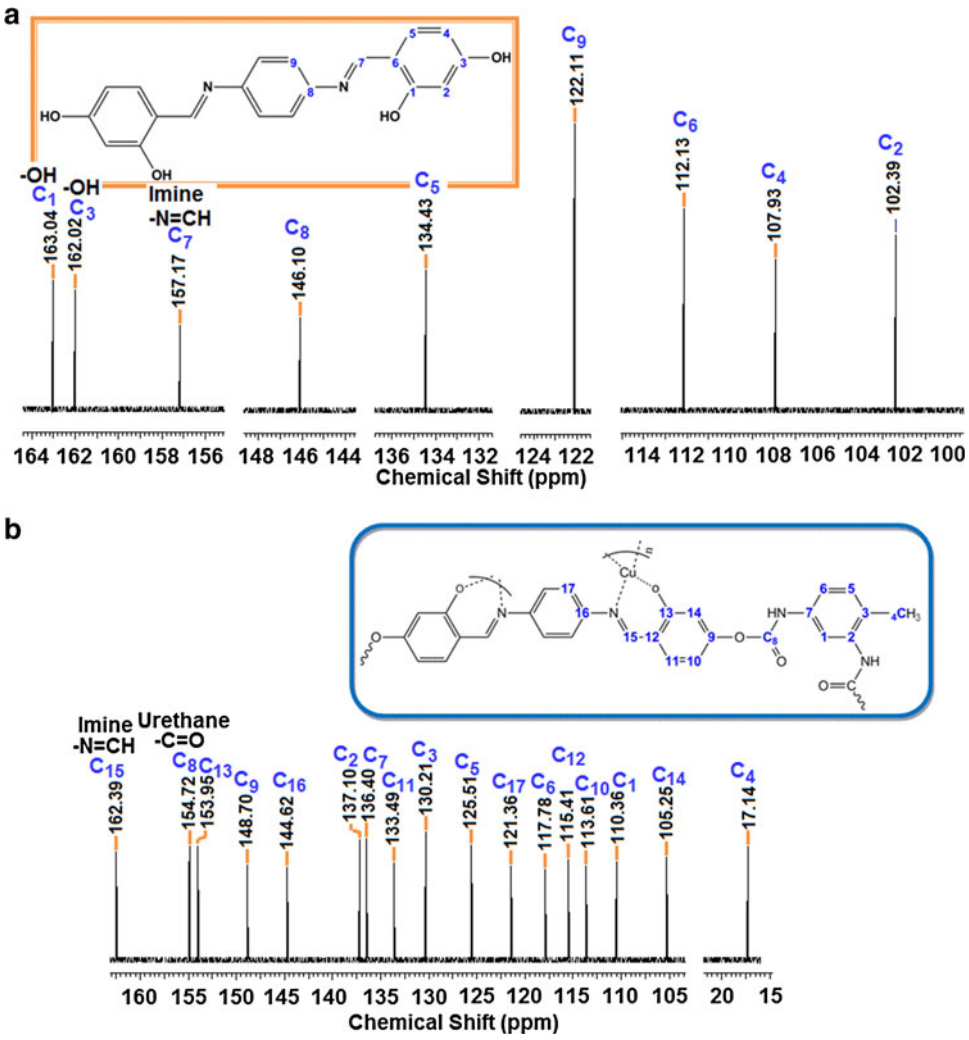

Fig. 2 ^{13}C-NMR spectra of 2,4-DHB–PDA (**a**) and PU-2,4-DHB–PDA–Cu (**b**)

observed results clearly confirm the formation of Schiff base, metal-containing Schiff bases and their poly(azomethine-urethane) derivatives.

^{1}H-NMR spectra of 2,4-DHB–PDA and PU-2,4-DHB–PDA–Cu are given in Fig. 1. Also, ^{1}H-NMR spectral data were summarized in Table 3. According to the Fig. 1 and Table 3, hydroxyl (–OH) and imine (–N=CH) protons are observed at 10.33 and 8.86 ppm for 2,4-DHB–PDA, respectively. Also, aromatic protons are observed between 6.32 and 7.45 ppm. According to the Table 3, hydroxyl (–OH) and imine (–N=CH) protons are observed at 9.96 and 8.42 ppm for 2,4-DHB–PDA–Cu. Aromatic protons are also observed between 7.67 and 6.39 ppm. According to ^{1}H-NMR spectrum of PU-2,4-DHB–PDA–Cu, hydroxyl (–OH) proton disappears due to urethane formation, urethane –NH and imine (–N=CH) protons are observed at 9.58 and 8.86 ppm, respectively. Also, methyl ($–CH_3$) proton is observed at 2.13 ppm and aromatic protons are observed between 6.43 and 7.98 ppm.

^{13}C-NMR spectra of 2,4-DHB–PDA and PU-2,4-DHB–PDA–Cu are given Fig. 2. The ^{13}C-NMR spectral data were also summarized in Table 3. According to Fig. 2a, hydroxyl (–OH) carbons and imine carbon (–N=CH) are observed at 163.04–162.02 and 157.17 ppm for 2,4-DHB–PDA, respectively. According to the Table 3, hydroxyl (–OH) and imine (–N=CH) carbons are observed at 163.70 and 160.26 ppm for 2,4-DHB–PDA–Cu, respectively. The hydroxyl (–OH) carbon (C_3) disappears due to metal complexes formation. In Fig. 2b, hydroxyl carbon (–C–OH) disappears due to urethane formation and imine (–N=CH) carbon is observed at 162.39 ppm for PU-2,4-DHB–PDA. ^{13}C-NMR spectra of PU-2,4-DHB–PDA at Fig. 2b also confirm the structure by the peaks observed at 154.72 ppm, respectively, which could be attributed to the urethane carbon. Also, methyl ($–CH_3$) carbon of PU-2,4-DHB–PDA–Cu is observed at 17.14 ppm. These results clearly show that the synthesized PAMUs are obtained with the proposed structures shown in Scheme 1.

3.2 Size Exclusion Chromatography

According to the SEC chromatograms, the number-average molecular weight (M_n), weight average molecular weight (M_w), and polydispersity index (PDI) values measured using RI detector (RID) are given in Table 4. According to these results, Mn, Mw and PDI values of metal-coordinated Schiff bases were calculated between 2,500–7,850, 3,100–11,300 and 1.222–1.439, respectively. According to the total values, 2,4-DHB–PDA–Cu, 2,4-DHB–PDA–Ni, 2,4-DHB–PDA–Pb and 2,4-DHB–PDA–Zn have nearly

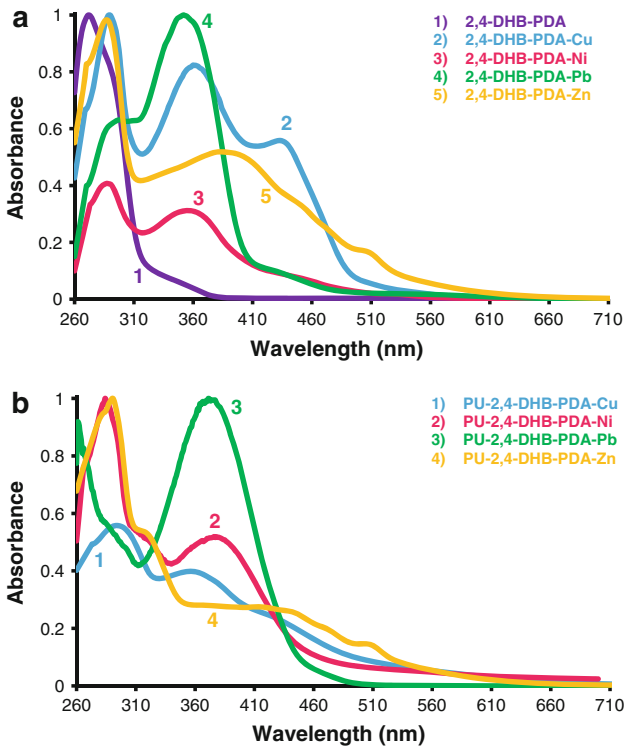

Fig. 3 UV–Vis spectra of Schiff base and its metal complexes (**a**) and poly(azomethine–urethane) derivatives (**b**)

Table 4 SEC analyses results of the synthesized compounds

Compounds	Molecular weight distribution											
	Total				Fraction I				Fraction II			
	Mn	Mw	PDI	%	Mn	Mw	PDI	%	Mn	Mw	PDI	%
2,4-DHB–PDA–Cu	7,850	11,300	1.439	100	7,510	11,200	1.491	88	10,350	11,700	1.130	12
2,4-DHB–PDA–Ni	2,500	3,100	1.240	100	1,100	1,320	1.200	92	18,550	23,320	1.257	8
2,4-DHB–PDA–Pb	7,100	9,100	1.282	100	1,900	3,700	1.947	85	36,400	39,800	1.093	15
2,4-DHB–PDA–Zn	3,600	44,00	1.222	100	2,700	3,400	1.259	88	10,250	11,700	1.141	12
PU-2,4-DHB–PDA–Cu	19,300	22,000	1.140	100	3,400	5,200	1.529	10	21,100	23,800	1.128	90
PU-2,4-DHB–PDA–Ni	13,400	15,700	1.172	100	4,700	5,200	1.106	5	13,900	16,200	1.165	95
PU-2,4-DHB–PDA–Pb	13,800	16,800	1.217	100	2,250	3,750	1.671	12	15,400	18,600	1.208	88
PU-2,4-DHB–PDA–Zn	23,000	24,000	1.043	100	2,750	3,160	1.149	10	25,200	26,400	1.048	90

23–32, 7–9, 20–26 and 10–13 repeated units, respectively. Similarly, Mn, Mw and PDI values of the PAMU-Ms were also calculated between 13,400–23,000, 15,700–24,000 and 1.043–1.217, respectively. According to the total values PU-2,4-DHB–PDA–Cu, PU-2,4-DHB–PDA–Ni, PU-2,4-DHB–PDA–Pb and PU-2,4-DHB–PDA–Zn have nearly 25–29, 18–21, 15–19 and 30–32 repeated units, respectively.

Table 5 Optical properties, electrochemical onset potentials and electronic energy levels of the synthesized materials

Compounds	UV–Vis			CV				
	λ (nm)	λ_{onset} (nm)	E_g (eV)[a]	E_{ox} (V)	HOMO (eV)[b]	E_{red} (V)	LUMO (eV)[c]	E'_g (eV)[d]
2,4-DHB–PDA	272, 351	376	3.30	1.0187	−5.41	−1.0144	−3.38	2.03
2,4-DHB–PDA–Cu	289, 361, 435	525	2.37	1.3307	−5.72	−1.5253	−2.86	2.86
2,4-DHB–PDA–Ni	287, 356, 453	461	2.69	1.3888	−5.78	−1.0181	−3.37	2.41
2,4-DHB–PDA–Pb	294, 353, 431	473	2.63	1.4739	−5.86	−1.3222	−3.07	2.79
2,4-DHB–PDA–Zn	287, 388, 507	554	2.24	1.4213	−5.81	−1.3387	−3.05	2.76
PU-2,4-DHB–PDA–Cu	295, 358, 437	589	2.11	1.3968	−5.79	−1.0619	−3.33	2.46
PU-2,4-DHB–PDA–Ni	284, 321, 383	555	2.34	1.6245	−6.01	−0.3387	−4.05	1.96
PU-2,4-DHB–PDA–Pb	262, 301, 378	517	2.40	0.8787	−5.27	−1.3446	−3.05	2.22
PU-2,4-DHB–PDA–Zn	291, 320, 442	623	1.99	1.3563	−5.75	−1.1989	−3.19	2.56

[a] Optical band gap

[b] Highest occupied molecular orbital

[c] Lowest unoccupied molecular orbital

[d] Electrochemical band gap

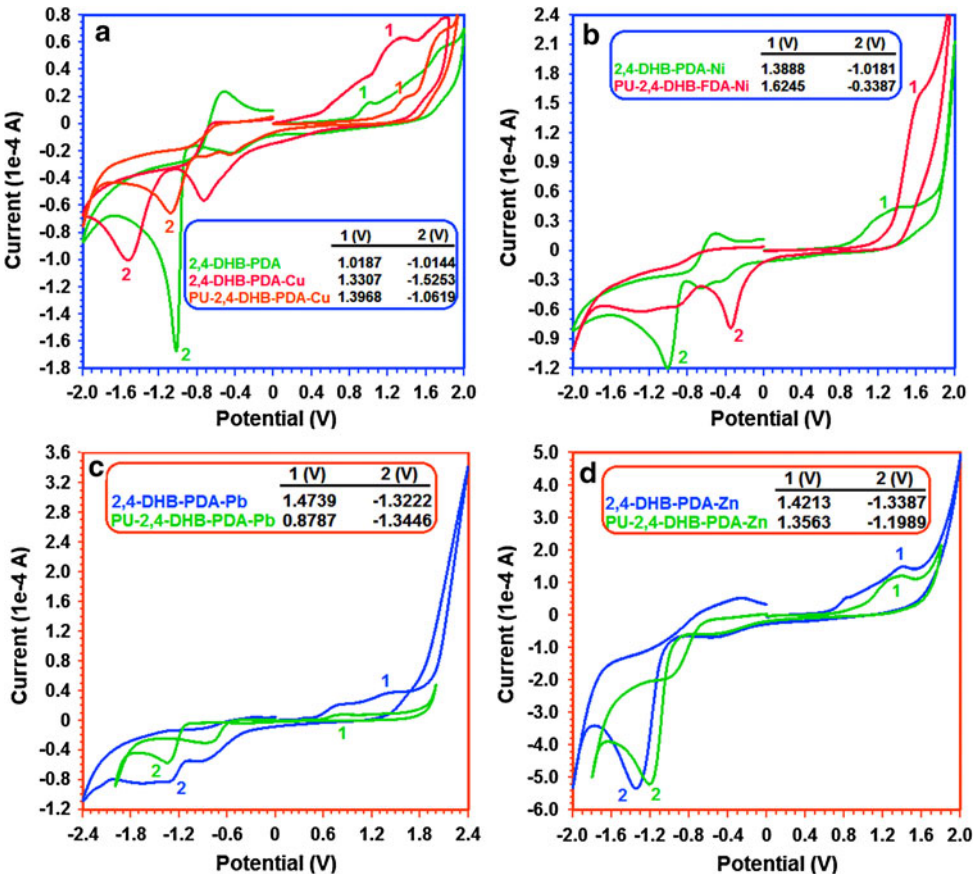

Fig. 4 Cyclic voltammograms of the obtained materials

3.3 Optical and Electrochemical Properties

UV–Vis spectra of the obtained materials are comparatively given in Fig. 3. According to Fig. 3a, $\pi \rightarrow \pi^*$ and $n \rightarrow \pi^*$ transition peaks of 2,4-DHB–PDA are appeared at 272 and 351 nm, respectively, due to the azomethine linkage in the structure. Similarly, these transition peaks of metal-coordinated Schiff bases are observed between 287–294 and 353–388 nm, respectively. Also, R-bands of metal-containing Schiff bases are appeared between 431 and 507 nm due to $d \rightarrow d'$ electron transitions of metal atoms in the structure [12]. According to the UV–Vis maxima of the PAMU-Ms, the absorption peaks are observed between 262 and 295 nm due to urethane linkage in the structures [17]. $n \rightarrow \pi^*$ transition peaks and R bands of the PAMU-Ms were also observed between 301–358 and 378–437 nm, respectively.

Optical band gap values could be obtained by using the following equation as in the literature [23], and shown in Table 4.

$$E_g = 1242/\lambda_{onset} \quad (1)$$

where λ_{onset} is the onset wavelength which can be determined by intersection of two tangents on the absorption edges. λ_{onset} also indicates the electronic transition start wavelength [27]. The calculated optical band gap values are shown in Table 5. As seen in Table 5, optical band gap of 2,4-DHB–PDA is calculated as 3.30 eV. The optical band gap of metal–coordinated Schiff bases and PAMU-Ms are calculated between 2.24–2.69 and 1.99–2.40 eV, respectively. According to the optical band gap values, PAMU-Ms have lower optical band gap value than Schiff base and its metal complexes due to the polyconjugated structures PAMU-Ms due to the polyconjugated structure decrease the Eg values. Also, these values are sufficient to make these PAMU-Ms electro-conductive materials [12].

The cyclic voltammograms of the materials are given in Fig. 4 and HOMO–LUMO energy levels and the electrochemical band gaps (E'_g) are summarized in Table 5.

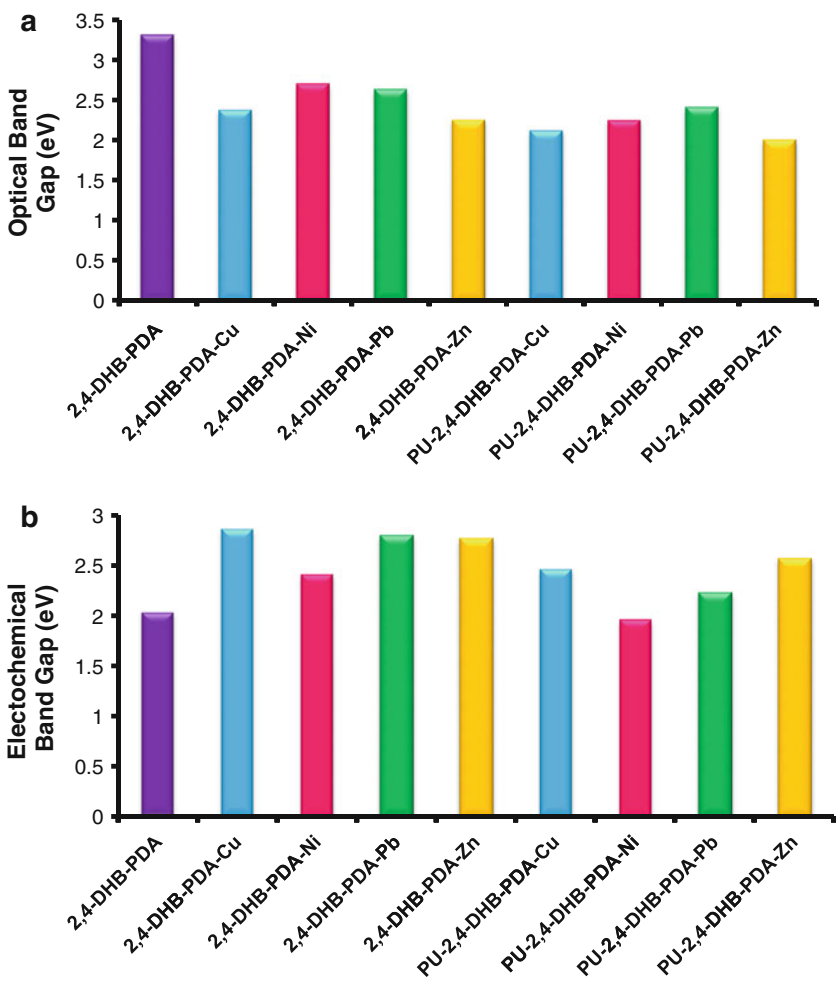

Fig. 5 Schematic representation of the optical (**a**) and the electrochemical band gap values (**b**)

These data were estimated by using the oxidation onset (E_{ox}) and reduction onset (E_{red}) values. The calculations were made by using the following equations [28]:

$$E_{HOMO} = -(4.39 + E_{ox}) \quad (2)$$

$$E_{LUMO} = -(4.39 + E_{red}) \quad (3)$$

$$E'_g = E_{LUMO} - E_{HOMO} \quad (4)$$

According to the CV results, HOMO–LUMO energy levels and electrochemical band gap value of 2,4-DHB–PDA was calculated as −5.41, −3.38 and 2.03 eV, respectively. The HOMO–LUMO energy levels and electrochemical band gap values of the metal-coordinated Schiff bases were calculated between −5.86 to (−5.72), −3.37 to (−2.86) and 2.41 to 2.86 eV, respectively. Also, the HOMO–LUMO energy levels and electrochemical band gap values of PAMU-Ms were calculated between −6.01 to (−5.27), −4.05 to (−3.05) and 1.96 to 2.46 eV, respectively.

The optical and the electrochemical band gaps are also shown schematically in Fig. 5. As seen Fig. 5 the order of optical and electrochemical band gaps (E_g) are as follows: PAMU-Ms > 2,4-DHB–PDA-Ms > 2,4-DHB–PDA. Obtained results indicate that PAMU-Ms have lower optical and electrochemical band gap values than their metal-coordinated Schiff bases. Lower band gaps facilitate the electronic transitions between HOMO–LUMO energy levels and make the PAMU-Ms more electro-conductive than the metal-coordinated Schiff bases [15].

3.4 Fluorescence Characteristics

Fluorescence measurements of PAMU-Ms are carried out using DMF. Measurements are also made for various concentrations to determine the optimal concentrations. Fig. 6 shows the excitation and emission spectra of PAMU-Ms in DMF. Also, Fig. 7 indicates the concentration-fluorescence intensity relationships of PU-2,4-DHB–PDA–Cu. The obtained results are also summarized in Table 6. These results clearly indicate that 2,4-DHB–PDA–Zn has higher excitation and emission intensity than the other metal-coordinated Schiff bases. Similarly, PU-2,4-DHB–PDA–Zn has higher excitation, and emission intensity than the other PAMU-Ms. These can be attributed due to the metal-to-ligand charge transfer (MLCT) and/or ligand-to-metal charge transfer (LMCT) [30]. As seen in Fig. 8, the optimum concentration to obtain maximal emission–excitation intensities is determined as 2.810×10^{-3} mg/L.

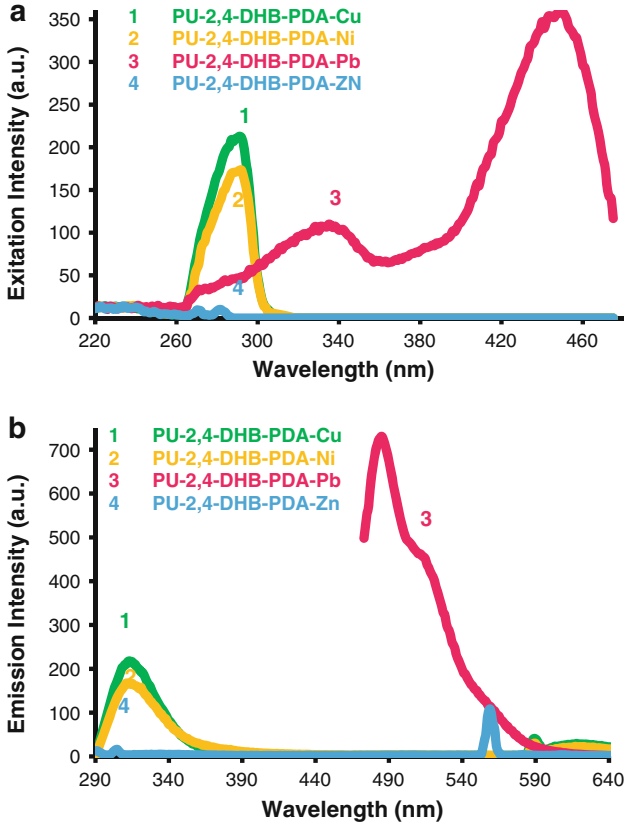

Fig. 6 Excitation (**a**) and emission spectra (**b**) of PAMU-M. *Slit width* λ_{ex}: 3 nm, λ_{em}: 3 nm

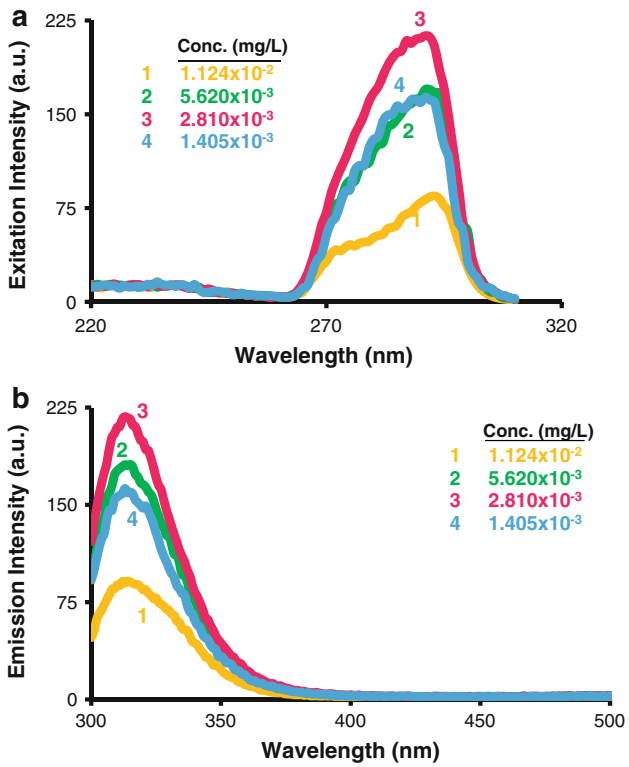

Fig. 7 Excitation (**a**) and emission spectra (**b**) of PU-2,4-DHB–PDA–Cu. *Slit width* λ_{ex}: 3 nm, λ_{em}: 3 nm

Table 6 Fluorescence spectral data of the synthesized compounds

Compounds	Conc. (mg/L)	λ^{a}_{Ex}	λ^{b}_{Em}	$\lambda^{c}_{max\ (Ex)}$	$\lambda^{d}_{max\ (Em)}$	I^{e}_{Ex}	I^{f}_{Em}
2,4-DHB–PDA	7.00×10^{-4}	277	546	271	558	52	67
2,4-DHB–PDA–Cu	3.50×10^{-4}	269	285	284	541	239	61
2,4-DHB–PDA–Ni	5.62×10^{-3}	305	347	346	613	283	58
2,4-DHB–PDA–Pb	$2. \times 10^{-3}$	279	294	270	561	14	115
2,4-DHB–PDA–Zn	2.81×10^{-3}	472	486	329	486	268	594
PU-2,4-DHB–PDA–Cu	2.81×10^{-3}	293	316	289	590	163	61
PU-2,4-DHB–PDA–Ni	2.81×10^{-3}	293	320	288	590	155	48
PU-2,4-DHB–PDA–Pb	2.81×10^{-3}	279	293	336	485	561	732
PU-2,4-DHB–PDA–Zn	2.81×10^{-3}	472	486	282	559	13	108

[a] Excitation wavelength for emission

[b] Emission wavelength for excitation

[c] Maximum excitation wavelength

[d] Maximum emission wavelength

[e] Maximum excitation intensity

[f] Maximum emission intensity

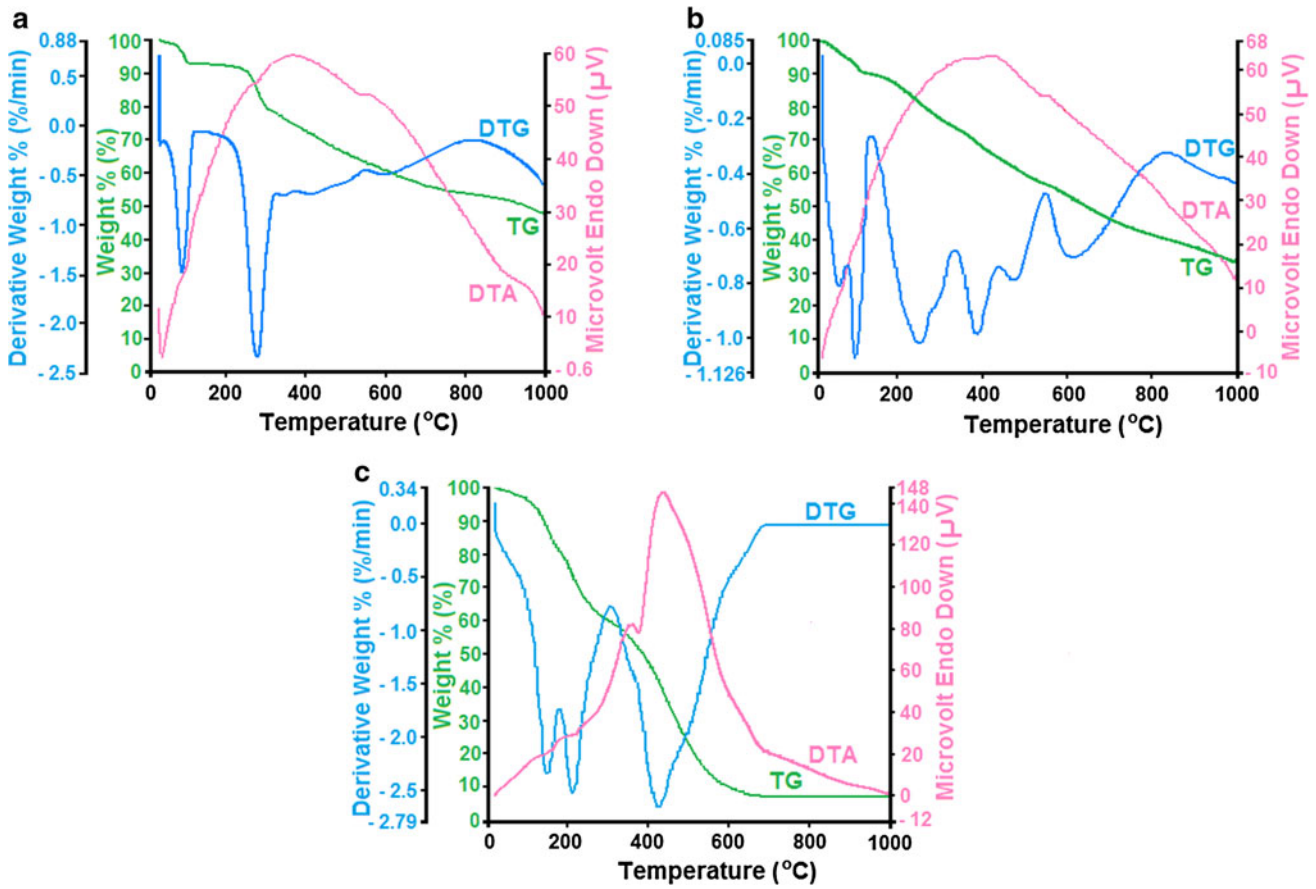

Fig. 8 TG–DTA curves of 2,4-DHB–PDA (**a**), 2,4-DHB–PDA–Ni (**b**) and PU-2,4-DHB–PDA–Ni (**c**)

Table 7 Thermal analysis data of the synthesized compounds

Compounds	TG					DSC	
	T^{a}_{on}	W_{max} T^{b}	T^{c}_{20}	T^{d}_{50}	Char at 1,000 °C (%)	T_g (°C)[e]	ΔCp (J/g °C)[f]
2,4-DHB–PDA	260	281	301	957	48	–	–
2,4-DHB–PDA–Cu	262	276, 433, 638, 870	282	876	44	164	0.332
2,4-DHB–PDA–Ni	211	255, 390, 480, 620	263	649	33	124	0.163
2,4-DHB–PDA–Pb	182	195, 232, 329, 962	307	920	33	119	1.934
2,4-DHB–PDA–Zn	207	222, 311, 578, 769	270	586	36	177	0.011
PU-2,4-DHB–PDA–Cu	192	218, 359, 600	213	552	38	122	0.154
PU-2,4-DHB–PDA–Ni	201	215, 429	179	392	28	138	0.082
PU-2,4-DHB–PDA–Pb	181	201, 285, 960	264	687	23	163	1.381
PU-2,4-DHB–PDA–Zn	212	240, 420, 582, 843	233	646	34	156	1.918

[a] The onset temperature

[b] Maximum weight temperature

[c] 20 % weight loss

[d] 50 % weight loss

[e] The glass transition temperature

[f] Change of specific heat during glass transition

3.5 Thermal Analyses

Thermal degradation properties of monomeric ligand, its metal complexes and its polychelates are determined by TG–DTG technique. TG–DTG–DTA curves of 2,4-DHB–PDA, 2,4-DHB–PDA–Ni and PU-2,4-DHB–PDA–Ni were shown in Fig. 8 and the obtained results were also summarized in Table 7. 2.0 and 4.0 % weight losses between 20 and 180 °C are attributed to losses of moisture or monomer [31]. According to the DTG curves 2,4-DHB–PDA and

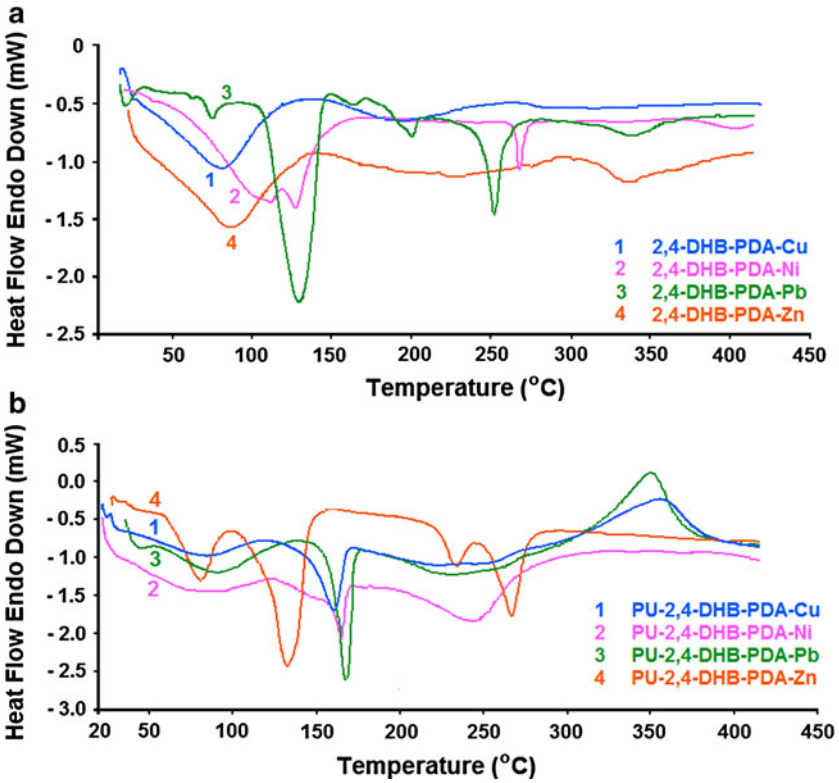

Fig. 9 DSC curves of metal-coordinated Schiff bases (**a**) and their poly(azomethine-urethane) derivatives (**b**)

PU-2,4-DHB–PDA–Ni thermally degrade in main three steps while 2,4-DHB–PDA–Ni degrades in main six steps. The first step probably indicates decomposition of coordinated water, the second step decomposition of uncoordinated part and the third step decomposition of coordinated part [22].

According to the Table 7, the onset temperature (T_{on}) of the Schiff base was measured as 260 °C. T20, T50 and char at 1,000 °C of 2,4-DHB–PDA were measured as 301, 957 °C and 48 %, respectively. According to Table 6, T_{on}, T20, T50 and char at 1,000 °C of the metal-coordinated Schiff bases are between 182–262, 270–307, 586–920 °C and 33–44 %, respectively. Also, T_{on}, T20, T50 and char at 1,000 °C of metal-coordinated PAMUs are between 181–212, 179–264, 392–687 °C and 23–38 %, respectively. According to these results, the obtained materials have quite high the onset temperature. Because of the fine thermal properties the they can be promising candidates for aerospace applications and they can be used to produce temperature-stable materials.

DSC curves of metal-coordinated Schiff bases and their poly(azomethine-urethane) derivatives are given in Fig. 9. Also, the obtained results from DSC traces are summarized in Table 7. According to the obtained DSC curves the glass transition temperatures (T_g) of the metal-coordinated Schiff bases and their poly(azomethine-urethane) derivatives are calculated between 119–177 and 122–163 °C, respectively.

4 Conclusions

Thermally stable PAMU-Ms were synthesized by step-polymerization reaction. TDI were used as co-monomer agent of the PAMU-Ms. According to fluorescence spectral data, 2,4-DHB–PDA–Zn and PU-2,4-DHB–PDA–Zn have higher excitation and emission intensity wavelength in DMF than the other metal-coordinated Schiff bases and PAMU-Ms. According to optical band gap values, the obtained PAMU-Ms have between 1.99 and 2.40 eV optical band gap values. Because of these values, they are sufficient to make these PAMU-Ms electro-conductive materials. According to the electrochemical band gap values, PAMU-Ms have between 1.96 and 2.56 electrochemical band gap values. Also, TGA results showed that the obtained Schiff base, metal-coordinated Schiff bases and their poly(azomethine-urethane) derivatives have high thermal stability. Consequently, because of the fine thermal properties the obtained materials can be promising candidates for aerospace applications and they can be used to produce temperature-stable materials.

Acknowledgments The authors would like to thank Government Planning Organization for the financial support (Project No: GPO2010K120710).

References

1. M. Yıldırım, İ. Kaya, Synth. Met. **161**, 13–22 (2011)
2. O.M.I. Adly, Spectrochim. Acta A. **95**, 483–490 (2012)
3. G. Tantaru, M.C. Popescu, V. Bild, A. Poiata, G. Lisa, C. Vasile, Appl. Organomet. Chem. **26**, 356–361 (2012)
4. A.A.A. Abou-Hussein, W. Linert, Spectrochim. Acta A. **95**, 596–609 (2012)
5. S.M. Ying, Inorg. Chem. Commun. **22**, 82–84 (2012)
6. L. Chakraborty, N. Chakraborty, T.D. Choudhury, B.V.N.P. Kumar, A.B. Mandal, N.V.S. Rao, Liq. Cryst. **39**, 655–668 (2012)
7. P. Sharma, A.P. Singh, Catal. Today **198**, 184–188 (2012)
8. T. Senapati, C. Pichon, R. Ababei, C. Mathonière, R. Clérac, Inorg. Chem. **51**, 3796–3812 (2012)
9. K. Huttinger, C. Forster, T. Bund, D. Hinderberger, K. Heinze, Inorg. Chem. **51**, 4180–4192 (2012)
10. H. Hatakeyama, N. Kato, T. Nanbo, T. Hatakeyama, J. Mater. Sci. **47**, 7254–7261 (2012)
11. F. Qiu, H. Xu, Y. Wang, J. Xu, D. Yang, J. Coat. Technol. Res. **9**, 503–514 (2012)
12. M.M. Rahman, A. Hasneen, H.D. Kim, W.K. Lee, J. Appl. Polym. Sci. **125**, 88–96 (2012)
13. M.Y.L. Chew, Constr. Build. Mater. **18**, 455–459 (2004)
14. O. Menes, M. Cano, A. Benedito, E. Giménez, P. Castell, W.K. Maser, A.M. Benito, Compos. Sci. Technol. **72**, 1595–1601 (2012)
15. İ. Kaya, M. Kamacı, Polimery **56**, 721–733 (2011)
16. G. Stoica, A. Stanciu, V. Cozan, A. Stoleriu, D. Timpu, J. Macromol. Sci. A **35**, 539–546 (1998)
17. K.R. Reddy, A.V. Raghu, H.M. Jeong, Polym. Bull. **60**, 609–616 (2008)
18. E.C. Buruiana, M. Olaru, B.C. Simionescu, Eur. Polym. J. **38**, 1079–1086 (2002)
19. S. Hasnain, N. Nishat, Spectrochim. Acta A **95**(2012), 452–457 (2012)
20. L. Chen, H. Xu, C.Z. Yang, T.D. Hu, Y.N. Xue, Polym. Adv. Technol. **8**, 335–338 (1997)
21. N. Senthilkumar, A. Raghavan, A.S. Nasar, Macromol. Chem. Phys. **206**, 2490–2500 (2005)
22. T. Ahamad, N. Nishat, S. Parveen, J. Coord. Chem. **61**, 1963–1972 (2008)
23. İ. Kaya, M. Kamacı, F. Arıcan, J. Appl. Polym. Sci. **125**, 608–619 (2012)
24. İ. Kaya, M. Yıldırım, A. Avcı, M. Kamacı, Macromol. Res. **19**, 286–293 (2011)
25. İ. Kaya, M. Yıldırım, M. Kamacı, Eur. Polym. J. **45**, 1586–1598 (2009)
26. S. Hasnain, N. Nishat, Spectrochim. Acta A **95**, 452–457 (2012)
27. E. İspir, Dyes Pigments **82**, 13–19 (2009)
28. İ. Kaya, M. Kamacı, Prog. Org. Coat. **74**, 204–214 (2012)
29. İ. Kaya, M. Yıldırım, M. Kamacı, A. Avcı, J. Appl. Polym. Sci. **120**, 3027–3035 (2011)
30. G.H. Eom, J.H. Kim, Y.D. Jo, E.Y. Kim, J.M. Bae, C. Kim, S.J. Kim, Y. Kim, Inorg. Chim. Acta **387**, 106–116 (2012)
31. İ. Kaya, A. Bilici, M. Saçak, J. Appl. Polym. Sci. **102**, 3327–3333 (2006)